Impact of potential climate change on crop yield and water footprint of rice in the Po valley of Italy

D. Bocchiola *

Politecnico di Milano, Dept. Of Civil and Environmental Engineering, L. da Vinci 32, 20133 Milano, Italy
EVK2CNR Association of Italy, San Bernardino 145, 24122 Bergamo, Italy

Received 28 November 2014
Received in revised form 28 July 2015
Accepted 31 July 2015

1. Introduction

Agriculture is a highly water consuming activity, heavily impacted by climate change, and potential reduction of harvest may lead to larger water requirements than now (Torriani et al., 2007; Bocchiola et al., 2013), and decline of *food security* (Adams et al., 1998; Olesen and Bindi, 2002; Olesen et al., 2007; Schmidhuber and Tubiello, 2007; Tubiello et al., 2007; Rost et al., 2008; Strzepek and Boehlert, 2010; Supit et al., 2010; Fader et al., 2011; Palazzoli et al., in press). Recently the concept of virtual water was introduced (Allan, 1993), *i.e.*, the water embodied in the production and trade of agricultural commodities, and assessment of *virtual water trade* is now used to quantify worldwide budget of water resources (Hoekstra and Hung, 2005). A key concept to virtual water quantification is the water footprint (WF) (Hoekstra, 2003a,b). Water footprint and *virtual water trade* are used to assess implications of worldwide trading strategies for *food security*, also pending climate warming (*e.g.*, Rosenzweig and Hillel, 1998; Easterling and Apps, 2005; Ferrero, 2006; FAO, 2009). The most relevant crops worldwide are cereals, especially rice *Oryza* L., wheat *Triticum* L., maize *Zea mais* L., requiring significant amounts of water for production, *i.e.*, rainfall and irrigation during summer (Tubiello et al., 2000; Torriani et al., 2007; Bocchi and Castrignanò, 2007; Confalonieri et al., 2009, 2011; Fava et al., 2010; Rossi et al., 2010). This in turn implies consider-able water footprint, and *virtual water trade* when crops are sold or bought (Bocchiola et al., 2013; Nana et al., 2014; Chapagain and Hoekstra, 2011). WF of crops is largely related to water requirements in their specific environment, and assessment of WF requires as accu-rate as possible estimates before large scale conjectures can be drawn. The same holds for analysis of climate change, which has global drivers, but local adaptation measures. Under transient climate change condi-tions, modified (increased, *e.g.*, Torriani et al., 2007) use of water by crops (per unit of yield) may cascade into modified (increased?) water footprint, requiring adaptation strategies. Modeling tools, includ-ing crop models, are necessary because they mimic crop production under specific climate conditions (*e.g.*, Richter et al., 2010), and can be later used to assess the potential effect of climate variations (*e.g.*,

* Politecnico di Milano, Dept. Of Civil and Environmental Engineering, L. da Vinci 32, 20133 Milano, Italy.
E-mail address: daniele.bocchiola@polimi.it.

Soussana et al., 2010). Before crop models are used however, their outputs need to be validated against measurements or estimates of the output variables (*e.g.*, Confalonieri and Bechini, 2004; Confalonieri et al., 2009), most notably crop productivity (Donatelli et al., 1997; Nana et al., 2014).

The possible effects of climate on agriculture may include i) physiological effect, *i.e.*, effect of CO_2 increase on plant respiration and photosynthesis cycles, ii) meteorological effects, *i.e.*, effects of temperature and rainfall changes (and irrigation requirement), and iii) effect of sea level rise and reduction of cultivable lands due to soil salin-ity increases (*e.g.*, Gornall et al., 2010). Doubling of CO_2 may increase photosynthetic rate by 30% to 100% in sensitive crop species, depending on temperature and water availability (Pearch and Bjorkman, 1983; Leuning, 1995; Jarvis et al., 1999). Species of type C3 (rice, wheat, *etc.*) react positively (*i.e.*, with increase of yield) to high CO_2. Type C4 crops (maize, sorghum, *Sorghum vulgare*, millet *Panicum miliaceum*, *etc.*) are less sensitive to changes in CO_2 (*e.g.*, Morrison, 1987, 1999). CO_2 further increases water use efficiency *via* decreased specific (*i.e.*, to leaf area) transpiration. Doubling CO_2 for C3 and C4 species may provide stomatal closure of about 40%, and a reduction of transpiration between 23% and 46% (Cure and Acock, 1987). Increasing temperatures may result in lon-ger potential growth season, and shorter maturation time (*e.g.*, Brouwer, 1988). Decreased precipitation, if not compensated for by (supplementary) irrigation, may lead to water stress. Climate change as projected for the 21st century may significantly alter crop production (Rosenzweig and Hillel, 1998; FAO, 2009). According to the Assessment Report 5, AR5 of the Intergovernmental Panel on Climate Change (IPCC) the effects of climate change on crop and food production are evident in several regions of the world, and the negative impacts of climate trends have been more common than positive ones (IPCC, 2013). By 2100 be-tween 5 million and 200 million additional people are expected to be at risk of hunger (Schmidhuber and Tubiello, 2007). While studies tack-ling future cereal production worldwide, or regionally are available, lit-tle investigation was devoted hitherto specifically to water footprint under climate change (see *e.g.*,modified irrigation in Tubiello et al., 2000, with WF not specifically addressed), and often it is assumed that unlimited water is available (*e.g.*, Masutomi et al., 2009 for a case study about rice). The specific aims here are to 1) investigate crop yield and water footprint in one specific area of Italy, for an important cereal locally (*i.e.*, rice), and 2) sketch future crop yield and water needs, usable for adaptation planning (under uncertainty) therein.

A simple hydrologically based, multi-year daily crop model called *PolyCrop* (henceforth, *PC*, Addimando et al., 2014; Nana et al., 2014) is used to study rice crop here. *PC* is based on the inclusion of a crop growth module into a semi-distributed (*i.e.*, grid based) hydrological model (Groppelli et al., 2011b; Bocchiola et al., 2011; Confortola et al., 2013; Addimando et al., 2014; Nana et al., 2014). Here, *PC* is used to study rice productivity, and water consumption in the Po valley (town of Landriano), in the Lombardia region of Italy. Po valley is among the most productive agricultural landscapes in Europe, and cropping there-in requires a large amount of water, being potentially at stake under fu-ture water stress. Therefore, one needs i) to assess accurately water consumption and rice yield under given climate conditions, and ii) to evaluate changes under future climate change.

Here to simulate the effects of future climate change, climate scenarios from two General Circulation Models (GCMs) (Community Climate System Model version 4 (CCSM4), European Centre HAmburg Model version 6 (ECHAM6)) from the IPCC panels, and three RCPs (RCP2.6, 4.5, 8.5) are downscaled, and fed to the *PC* model to simulate rice production and water use (as in *e.g.*, Palazzoli et al., in press, for a case study in Nepal). Two reference periods are studied, at half century (2040–2046), and end of the century (2080–2086), and three key variables were considered, namely temperature, precipitation, and CO_2.

The manuscript is structured as follows. In Section 2 the case study site of Landriano (in Pavia province, Fig. 1) is presented, where rice yield data lumped on Pavia province were made available by the Italian Institute of Statistics (ISTAT) for seven years (2006–2012). The *PC* model set-up is then described. Then, water footprint of rice in the area is defined, and the estimation method provided. The method for projection under climate change scenarios is described, and a correlation analysis is introduced, used to highlight the climate variable mostly influencing cropping, and water use. In Section 3 the Results are pre-sented. Modeling accuracy using *PC* is addressed, and present water footprint of rice in Landriano reported. Then projected future changes in rice yield and water use are shown, together with results from the correlation analysis. In Section 4 the results are discussed. The modeling

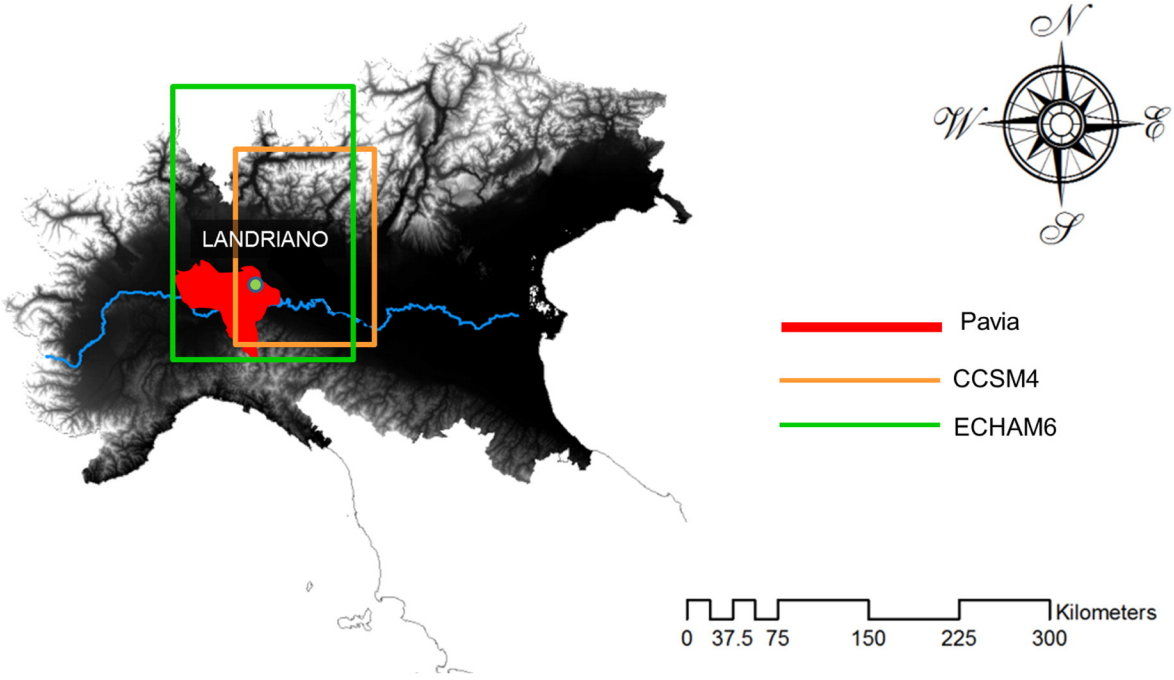

Fig. 1. Case study area. Landriano in the Pavia province of Italy (in red). Footprint of CCSM4 and ECHAM6 models reported. (For interpretation of the reference to color in this figure legend, the reader is referred to the web version of this article.)

performance of the *PC* model, and the estimated water footprint of rice are benchmarked *vs* the results of similar studies worldwide. The uncertainty of crop yield and WF projections in response to uncertain climate evolution is discussed, and whenever possible future crop yield and WF are compared against results from similar studies. Limitations of the study, and possible developments and adaptation strategies are then reported. Then conclusions are drawn.

2. Materials and methods

2.1. Study area

The Lombardia region (Fig. 1) is nested in the Po valley of Italy, displaying farming areas over 45% of the catchment (and 2200 km^2 covered with rice fields). The major crops are wheat, maize, barley (*Hordeum vulgare* L.), sugar beets (*Beta vulgaris* L.), and rice (see Bocchiola et al., 2013). Pavia province (Fig. 1) is laid within the southern, less rainy end of Lombardia region, covering ca. 2970 km^2, out of which 800 cultivated with rice, *i.e.*, the first province of Italy for rice production. The average altitude of the Pavia province is 144 m asl, and it belongs to an area with continental/warm climate (Köppen–Geiger, *e.g.*, Peel et al., 2007), with average year round tem-peratures of +12–14 °C and average rainfall of 650–700 mm. Winter is cold (+2.5 °C on average) and summer is hot (+23 °C on average), with wind speed generally low. Rainfall regime is bimodal, highest in fall, and lower in early spring. Landriano town, *ca.* 6000 inhabitants, has a surface of 15.5 km^2, and an average altitude of 88 m asl. Soil is coarse silty loam down to about 30 cm, and finer silty loam layer to about 70 cm. The water table is about 1–5 m under the surface. Irriga-tion strategies of local farmers were gathered *via* interviews. Rice fields are watered in the first days of April, until harvest at the end of August, with a total amount of ca. 500 mm (Table 1). A constant water layer (ca. 50 mm in depth) is maintained for rice cropping. Sowing date is fixed at April 20, and this date was used here normally. In 2009, the ISTAT data displayed larger yield than usual, likely given by high temperatures, and possibly anticipated sowing date, which was then taken 15 days earlier.

2.2. Data base

In Landriano an automatic weather station (AWS) of the regional environment protection agency ARPA (Agenzia Regionale Protezione dell'Ambiente) is available. However, the data therein were not complete, and crop modeling was not feasible. A data base delivered under the project Crop Growth Monitoring System (CGMS) was then used, developed by the Monitoring Agricultural ResourceS (MARS) unit of the Joint Research Centre (JRC), and suited for agricultural simulation (Confalonieri et al., 2009). The meteorological data in the grid points $\varphi = 45°18'$ and $\lambda = 9°15'$ were used. Comparison against ARPA data whenever available showed good agreement. Average (2006–2012) yearly rainfall was $P_{av} = 673$ mm, and average yearly temperature $T_{av} = 13$ °C. Given the lack of data, radiation was calculated from topography and date, and modified to account for cloud cover depending on daily precipitation.

Table 1
Landriano. Typical irrigation calendar for rice, as per the farmers' interviews.

Date	Irrigation [mm]
April 2	30
April 15	55
May 5	120
June 20	80
July 1	100
July 13	20
August 4	50
August 22	20

GCMs are physically based models providing meteorological variables for impact assessment. Two coupled GCM models were used here (Fig. 1, Table 2), namely CCSM4 (Gent et al., 2011), and ECHAM6 (Stevens et al., 2013). The Representative Concentration Pathways (RCPs) adopted in the IPCC's Fifth Assessment Report (AR5) describe projections of the components of radiative forcing, *i.e.*, the change in the net balance between incoming and outgoing radiation in the atmo-sphere, depending on changes in atmospheric composition (IPCC, 2013). The scenario set is composed of four RCPs (RCP2.6, RCP4.5, RCP6.0, and RCP8.5), named according to their radiative forcing in 2100 (+2.6, +4.5, +6.0 and +8.5 W m^{-2}, respectively). Here, three RCPs (2.6, 4.5, 8.5) were selected, with RCP4.5 and RCP6.0 being some-what similar. Downscaling of the GCM output of precipitation and tem-perature was pursued to obtain more representative data at the spatial scale of analysis (Groppelli et al., 2011a; Bocchiola et al., 2013; Palazzoli et al., in press). Daily precipitation was downscaled using the Stochastic Space Random Cascade (SSRC) approach. This involves two main steps, namely correction of *Bias*, and disaggregation. Model calibration was carried out using the CGMS daily data during 2006–2012. Downscaling of temperatures was achieved comparing seasonal means from CGMS during 2006–2012 against mean values derived from the local data. The difference (ΔT) between average values was used to correct GCMS temperatures. CO_2 was taken as a constant, from each RCP, and period (RCP2.6, CO_2 = 443, 426 ppm, RCP4.5, CO_2 = 487, 534 ppm, RCP8.5, CO_2 = 540, 845 ppm, for 2040 and 2080, against CO_2 = 370 ppm presently).

2.3. PolyCrop model

The spatially semi-distributed *PC* model was used, obtained by nesting a crop growth module into a spatially distributed hydrological model (Addimando et al., 2014; Nana et al., 2014). The crop growth module simplifies presently available models, such as *CropSyst* (Stöckle et al., 2003). The hydrological model provides soil water content, used by the crop module to simulate growth. In turn, the growth module provides values of *LAI* used by the hydrological model to calcu-late transpiration, fraction of vegetated soil, and modified soil water content. At present, lateral flows are neglected, valid for flat areas, with little lateral redistribution, as in our case study areas. Only one soil layer was considered for simplicity. The hydrological model is based upon a water budget equation delivering soil water storage S [mm] at two consecutive time steps $(t, t + \Delta t)$

$$S^{t+\Delta t} = S^t + P\Delta t + I\Delta t + ET\Delta t - Q_g\Delta t - Q_s\Delta t. \quad (1)$$

Here at daily scale P is rainfall [mm d^{-1}], I is irrigation [mm d^{-1}], ET [mm d^{-1}] is (actual) evapotranspiration, Q_g [mm d^{-1}] is groundwater discharge, and Q_s [mm d^{-1}] is overland flow (occurring for soil saturation). The daily growth in biomass is the minimum value between a water (transpiration) dependent growth (G_{TR}), and a solar radiation dependent growth (G_R)

$$G_{TR} = \frac{T_{eff} BTR}{VPD}; G_R = L_{tbc}\, PAR\, f_{PAR}\, T_{\lim} \quad (2)$$

with G_{TR} [kg m^{-2} day^{-1}] transpiration dependent biomass growth, T_{eff} [m day^{-1}] effective (actual) transpiration, *VPD* [kPa] average vapor

Table 2
Main properties of the GCM models used here.

Model	Research Centre	Grid size [°]	n. cells	layers
CCSM4	Nat. Center for Atmospheric Research, USA	1.25° × 1.25°	288 × 144	26
ECHAM6	Max Planck Institute for Meteorology, GER	1.875° × 1.875°	192 × 96	47

pressure deficit, *BTR* [kPa kg m^{-3}] biomass transpiration coefficient, G_R [kg m^{-2} day^{-1}] radiation dependent biomass growth, L_{tbc} [kg MJ^{-1}] light to biomass conversion coefficient, *PAR* [MJ m^{-2} day^{-1}] photosyntetically active radiation, f_{PAR} [.] fraction of incident *PAR* intercepted by canopy, and $T_{\lim}$ temperature limitation factor [.]. Full nutrient availability was assumed, and nitrogen budget was not simulated (*i.e.*, N is not a limiting factor). Preliminary investigation indicated full availability of nutrients in Landriano. Crop growth stages are based upon accumulation of thermal time (or degree–days) during the growth season (Stöckle and Nelson, 1999). In the presence of vegetation, evapo-transpiration depends on the *LAI*, iteratively calculated for each day of the simulation. The effective transpiration depends upon the daily veg-etation growth, and its vegetative stage (Stöckle et al., 1994), as

$$f_{PAR} = 1 - \exp(-kLAI_{cum}), \quad (3)$$

and

$$T_{eff} = 86,400\frac{C}{1.5(\Psi_s - \Psi_x)}, \quad (4)$$

where k [.] is the extinction coefficient for solar radiation, LAI_{cum} [m^2 m^{-2}] is the cumulated leaf area index until the day when f_{PAR} is calculated, C [kg s m^{-4}] is the root conductance, Ψ_s [J kg^{-1}] is soil water potential, depending upon soil water content (Campbell, 1985), Ψ_x [J kg^{-1}] is leaf water potential, 86,400 is the number of seconds per day, and 1.5 is a factor converting root conductance into hydraulic conductance. To model crop growth dependence *vs* CO_2 we mimicked *CropSyst*, where two approaches are adopted, namely i) Monteith's (1977) approach, which modifies radiation dependent growth G_R in Eq. (2), and ii) the Tanner and Sinclair (1983) approach, which modifies transpiration dependent biomass growth G_{TR} in the same equation. Modified versions of these approaches, tailored on the bases of recent experiments, are implemented in *CropSyst* (Stöckle et al., 1992, 2003; O'Leary et al., 2015), and were adopted here, as follows

$$G_{R,CO_2} = G_R C_{R,CO_2} = G_R \frac{(-1.7/(350(1-1.7))CO_2\,1.7)}{(-1.7/(350(1-1.7))CO_2 + 1.7)}$$
$$G_{TR,CO_2} = G_{TR} C_{TR,CO_2} = C_R/((\delta + (\gamma 336/300))/(\delta + \gamma((36CO_2)/(350C_R) + 300)/300)), \quad (5)$$

with δ [kPa °C^{-1}] psychrometric constant, and γ [kPa °C^{-1}] slope of the saturated vapor pressure–temperature curve. For instance, for CO_2 = 350, and 650 ppm, one has C_{R,CO_2} = 1, and 1.23, respectively. The *PC* model is used here in a point-wise version, given the limited size of the area (see Addimando et al., 2014 for a distributed application).

2.4. Model setup

The model requires series of daily precipitation, maximum and min-imum temperature, and solar radiation. Soil properties and use were made available by the regional agency for agriculture and forest services ERSAF (Ente Regionale per i Servizi all'Agricoltura ed alle Foreste). Main soil properties are given in Table 3. Further information about rice is necessary for *PolyCrop* set up. Some parameters were taken from former studies (Confalonieri et al., 2006) and are reported in Table 4. Some parameters are site-specific, and it was necessary a calibration phase against yield data (Table 5), by tuning within their documented range of variability, as provided *e.g.*, by the *CropSyst* user manual (Stöckle and Nelson, 1999). *PolyCrop* allows different irrigation strategies, name-ly i) no irrigation (NO), ii) automatic irrigation (AU), *i.e.*, on demand, and iii) manual irrigation (MA), according to farmers' scheduling (Table 1). In AU mode, whenever the water layer is shallower than a tar-get depth, water is added. Given that the approximate irrigation sched-uling may not be representative of the real behavior of farmers in the area, we decided to also use AU mode for calculations. Also, use of AU option may demonstrate the potential of automatic irrigation for rice cropping. Here, simulations were carried out for the reference period (2006–2012, henceforth control run (CR)) in three ways. First, MA irri-gation was used, to carry out the model's validation under the actual (as reported by farmers) irrigation schedule. Secondly, the NO irrigation option was adopted (*i.e.*, without irrigation, or rain fed cropping), to test crop yield whenever irrigation would not be available. Third, the AU mode was adopted. Notice that rice cropping here occurs under flooded conditions, most notably to dampen temperature jumps, and to avoid weeds (Cabangon et al., 2004; Confalonieri and Bocchi, 2005; Confalonieri et al., 2006, 2009), and flooding water needs be accounted for when calculating water footprint (Chapagain and Hoekstra, 2011). In Landriano, a water layer of ca. 50 mm is kept on the rice field from sowing to end of growth.

To account for the effect of flooding upon rice growth, water temper-ature was estimated as in Confalonieri et al. (2005), by an empirical al-gorithm that evaluates daily max and min water temperatures taking a weighted average of air maximum and minimum temperatures cen-tered on a three day window. Temperature outside water was assumed to linearly vary until the air value, at 2 m above the water layer (Confalonieri et al., 2005). Then, temperature at the meristematic apex

Table 3
Landriano. Main soil properties for set-up of *PolyCrop*.

Variable	Range	*PC*
Active soil depth [m]	–	0.85
Percentage of sand into soil [%]	0–100	12
Percentage of silt into soil [%]	0–100	65
Percentage of clay into soil [%]	0–100	23
Soil water content at wilting point θ_w [.]	0.01–0.25	0.13
Soil water content at field capacity θ_l [.]	0.1–0.35	0.31
Soil water content at saturation θ_s [.]	0.2–0.5	0.50

Table 4
Landriano. Agricultural parameters (from literature) for rice growth simulation using *PolyCrop*.

Growth parameters	Landriano
Biomass/transpiration coefficient [kPa kg m^{-3}]	5
Conversion light/biomass [g MJ^{-1}]	3
Real/potential transpiration, end of leaf growth [.]	0.8
Real/potential transpiration, end of root growth [.]	0.5
Mean daily temperature optimal growth, T_{opt} [°C]	28
Max daily water consumption, W_{maxd} [mm d^{-1}]	10
Leaf water potential, Ψ_x [J kg^{-1}]	−1200
Leaf water potential at wilting, Ψ_w [J kg^{-1}]	−1800
Morphology	
Max root depth, d_{Rmax} [m]	0.85
Initial green area index [m^2 m^{-2}]	0.01
Max leaf area index, LAI_{max} [m^2 m^{-2}]	7
Fraction LAI_{max} at maturity [.]	0.5
Specific leaf area *SLA* [m^2 kg^{-1}]	27
Leaf duration [°C d]	700
Extinction coefficient of solar radiation [.]	0.5
Evapotranspiration coefficient K_c [.]	1.05
Phenology	
Base temperature [°C]	12

Table 5
Landriano. Calibration parameters for rice growth simulation using *PolyCrop*.

Parameters	Range	Landriano
Specific leaf area [m^2 kg^{-1}]	20–60	27
Partition stem/leaf [.]	1–10	3.1
Degree–day emergence [°C d]	0–300	80
Degree–day flowering [°C d]	300–1500	975
Degree–day maturity [°C d]	1000–2500	1400
Threshold temperature [°C]	0–10	10
Cutoff temperature [°C]	33–40	40

height was used for simulating the processes related to plant develop-ment. Apex height is taken according to the TRIS micro-meteorological model (Confalonieri et al., 2005, 2009), depending on a Development Stage decimal code function of the degree–day. Max height is set to 100 cm (Confalonieri et al., 2009). Canopy temperature is calculated as the average value of temperature inside and outside water, from the ground to the canopy height, and used for simulating thermal limi-tation to photosynthesis (Confalonieri et al., 2009). For the purpose of evaluating water footprint presently, and under climate change, it is used the AU irrigation mode. In fact, under such mode, the exact amount of water necessary for cropping is evaluated. The use of MA mode (with present values) may provide lack of water, so in the future a different (larger) amount of water may be necessary.

2.5. Water footprint

Water consumption for cropping is calculated *via* the concept of green and blue water footprint (Hoekstra, 2003a,b; Hoekstra and Chapagain, 2008; Rost et al., 2008; Fader et al., 2011). This is a numerical index (either dimensional, *e.g.*, mm, or specific, *e.g.*, kg kg^{-1}), expressing the amount and origin of water used for the production of a given good. In agreement with Rost et al. (2008) two water footprint indicators were used here, namely i) green water footprint (WF_G), and ii) blue water footprint (WF_B). Green water footprint is the consumption of water stored in the ground as a result of precipitation. WF_G was eval-uated by comparing evapotranspiration during the growth season (ET_g), as simulated by the model, against the cumulative precipitation during the growing season (P_g)

$$\begin{array}{l} ET_g = E_{s,g} + T_{c,g} \\ \text{if } ET_g \geq P_g \quad WF_G = P_g \\ \text{if } ET_g < P_g \quad WF_G = ET_g \end{array}, \tag{6}$$

where $E_{s,g}$ is soil evaporation and $T_{c,g}$ is transpiration from the crop during the growing season. Accordingly, when evapotranspiration during the growth season exceeds precipitation, green water footprint equals precipitation. Conversely, when P_g is higher than ET_g, WF_G equals ET_g, *i.e.*, in the case in which abundant precipitation evapotranspiration is entirely sustained by precipitation (however this is never the case in Landriano for rice). The water in rice biomass was also neglected, which is however small against ET_g. Accordingly, blue water footprint refers to the consumption of water the aim of which is to fulfill ET_g (Mom, 2007; Rost et al., 2008; Fader et al., 2011). WF_B was evaluated here as

$$\begin{array}{l} \text{if } ET_g \geq P_g \quad WF_B = ET_g - P_g \\ \text{if } ET_g < P_g \quad WF_B = 0 \end{array}. \tag{7}$$

When P_g is larger than ET_g (*i.e.*, rainfall is larger than evapotranspiration), no blue water footprint is necessary. Conversely, when ET_g is larger than P_g (and rainfall is not enough to sustain evapotranspiration), blue water footprint occurs, and it is quantified as the difference between ET_g and P_g. Given the requirement for a water layer for rice flooding, more water is added than is necessary to meet potential evapotranspiration, which may provide runoff, percolation, or increased soil moisture. Albeit such water cannot be considered as a waste, it is not strictly speaking necessary for crop growth, and can therefore be considered as an excess of irrigation. To quantify this facet, an irrigation water footprint WF_I was introduced here as

$$WF_I = \sum_{i=1}^{n} I_i, \tag{8}$$

i.e., the cumulated amount of water upon the *n* irrigation events, both under the MA and AU irrigation schemes. Chapagain and Hoekstra (2011), when investigating seasonal water footprint of rice cropping worldwide, included (in addition to crop evaporative demand) the amount of water necessary to saturate the soil initially (with a standard value of 200 mm), and to maintain flooding (with a standard value of 100 mm), plus percolation water (lost underground, with a standard value of 2.5 mm d^{-1}). Here, the water budget of the soil, and the amount of water provided for irrigation (MA, and AU, including initial soil saturation, and flooding) were calculated on a daily basis, so it was not necessary to account for these three terms separately. Notice

Table 6
Statistics of crop yield and goodness of fit under the MA, NO, and AU modes.

	Crop yield statistics		Goodness of fit		
	E[Y] [ton ha^{-1}]	DEVST[Y] [ton ha^{-1}]	$Bias_{\%}$	*RMSE* [ton ha^{-1}]	$RMSE_{\%}$
ISTAT	6.17	0.34	–	–	–
MA	6.23	0.48	1%	0.6	10%
NO	4.72	0.66	−23%	1.6	25%
AU	6.32	0.44	3%	0.6	10%

Mode	MA			NO	
	WF_G	WF_B	WF_I	WF_G	WF_B
Water footprint WF [mm] CR period					
E[WF]	384.9	471.7	598.2	384.9	*100.2*
DEVST[WF]	56.2	68.8	23.1	56.2	*90.6*

Mode	AU			
	WF_G	WF_B	WF_I	WF_G^*
Water footprint WF [mm], WF [kg kg^{-1}] CR period*				
E[WF]	384.9	464.3	605.1	612.6
DEVST[WF]	56.2	64.0	58.1	105.5
WF [kg kg^{-1}], WF^P [.] CR period*				
	WF_B^*	WF_I^*	WF_B^P	WF_I^P
E[WF]	735.6	960.1	1.25	1.60
DEVST[WF]	94.7	108.3	0.37	0.27

The mean and standard deviation of $WF_{G,B,I}$ during the CR period are also reported. WF_B in *italics* indicates use of previous soil moisture under NO irrigation mode. Also specific WF^*, and relative WF^P water footprint are reported for the AU mode ($WF_G^P = 1$ always, not reported).

here that water footprint is not considered as a term of the water budget in Eq. (1), or of the crop growth model in Eqs. (2)–(5). Instead, the terms WF_G, WF_B, and WF_I are indicators drawn from variables included in (P_g, I_g), or calculated from (ET_g) the *PolyCrop* model, that directly highlight the use of water for the purpose of cropping, also emphasizing water origin (*i.e.*, from rainfall, or irrigation), and give lumped information of water needs for managers, and to sketch adaptation strategies. Also, *specific* (green or blue) water footprint (WF^*) was estimated here, *i.e.*, the amount of water in kg necessary to produce 1 kg of harvested yield *Y*, namely

$$WF_{G,B,I}{}^{*} = \frac{WF_{G,B,I}}{Y}, \tag{9}$$

together with *relative* (green or blue) water footprint WF^P, *i.e.*, the ratio of water footprint to P_g

$$WF^{P}_{G,B,I} = \frac{WF_{G,B,I}}{P_g}. \tag{10}$$

Here, gray water footprint (Mekonnen and Hoekstra, 2011), *i.e.*, the water volume required to dilute pollutants such as fertilizers, was neglected. Calculation of gray water footprint requires mass budget of fertilizers, and possibly validation against samples, not carried out here as reported.

2.6. Simulation of crop yield and water footprint under future climate change

To simulate crop yield and water footprint under climate change, the downscaled outputs of precipitation, temperature, and CO_2 from the adopted GCMs were fed to the *PC* model, under AU irrigation mode (with a constant water layer of 50 mm), and crop growth was simulat-ed. Crop yield, harvest date (D_H), and the water footprint indicators above were then recalculated. Here, the reference period CR (with ISTAT yield data available) was of seven years, so future reference periods of the same length were taken, namely 2040–2046 (shortly 2040), and 2080–2086 (shortly 2080), for better comparability.

2.7. Correlation analysis of crop yield and water footprint against climatic drivers

A correlation analysis was used to highlight the potential effect of CO_2, and climate variables (*P*, *T*) on crop yield, and water use during the growth period. Specifically, average values of *Y*, D_H, WF_B, and WF_I (not WF_G, substantially matching rainfall) were tentatively correlated against CO_2, temperature during growth season (T_g), and precipitation in the same season (P_g). A preliminary analysis indicated that the seasonal values of *T* and *P* influenced differently cropping behavior, so spring (AMJ), and summer (JAS) values were taken separately. Albeit the growth period changes slightly from year to year (namely with start in April 20th, the earliest harvest date at August 11th in 2007, and the latest at August 25th in 2008), and shortens in the future (see Section 3.3) the seasonal weather variables as calculated should be rep-resentative of changes in crop productivity and water use.

3. Results

3.1. Modeling accuracy

Several runs of *PC* were carried out, to obtain yield data coherent with those given by ISTAT. In Table 5, calibration parameters of *PC* are displayed, and in Table 6 calibration results reported. Soil water balance, and crop growth were simulated during January 1st 2006 to December 31st 2012. In Fig. 2a, the best simulation is reported, in terms of productivity (dry biomass), against ISTAT data. Calibration was pursued by manually changing the calibration parameters, and most notably degree–day factors, and cutoff temperatures. Manual irrigation MA (Table 1, with *ca.* 500 mm of water in total) was considered for calibra-tion. The calibration provided acceptable agreement (average error $Bias_{\%} = 1\%$, random mean square error $RMSE = 0.6$ ton ha^{-1}, percentage random mean square error $RMSE_{\%} = 10\%$). Simulation under NO irrigation mode provides large underestimation of crop yield ($Bias_{\%} = -23\%$, $RMSE = 1.6$ ton ha^{-1}, $RMSE_{\%} = 25\%$), indicating that under rain fed conditions crop yield is sensibly lower (ca. 75% or so) than with irrigation. Automatic irrigation again provides good agreement against ISTAT data ($Bias_{\%} = 3\%$, $RMSE = 0.6$ ton ha^{-1}, $RMSE_{\%} = 10\%$). Here, sensitivity analysis of the parameters, which may be of interest for assessing the model's robustness, is not explicitly carried in order to focus upon water use, and future projections.

3.2. Estimated water footprint in the reference period

Estimated water footprint in the CR period calculated by Eqs. (5)–(7) is reported in Fig. 2b, for both MA, NO, and AU irrigation modes, the latter chosen as a reference for climate change effect assessment as re-ported (CR simulation). Also statistics (mean, and standard deviation) of WF values under each mode are reported in Table 6. WF_G is equal for all irrigation modes, and coincides with precipitation (see Eq. (6), case $ET_g \geq P_g$) *i.e.*, rainfall is entirely used for crop growth, and clearly changes every year (max 457.7 mm in 2012, min 308.6 mm in 2008). WF_B is similar for MA and AU (on average 472 mm, and 464 mm for MA and AU, respectively). Yearly changing WF_B depends on changes in WF_G (*i.e.*, in rainfall), and normally the larger the WF_G, the smaller the WF_B. In each year high/low WF_B for MA also implies high/low WF_B for AU, because no matter the method, when large irrigation is needed WF_B increases. Accordingly max WF_B is in 2011 for both MA, and AU (Fig. 2b, 598.0 mm, and 580.8 mm, respectively), and min WF_B occurs in 2011 again for both MA, and AU (Fig. 2b, 381.0 mm, and 382.5 mm, respectively). WF_I, *i.e.*, total irrigation is also similar for MA, and AU (on average 598 mm, and 605 mm for MA and AU, respectively) albeit variable from year to year (*e.g.*, in response to high temperatures, and low rainfall, with a max in 2006, 640.6 mm, and 718.6 mm for MA, and AU respectively, and a min in 2009 for MA, 575 mm, and in 2010 for AU, 540.1 mm). However, the use of AU irrigation provides slightly higher yield, as seen in Fig. 1, and a constant water layer of *ca.* 50 mm, whereas MA irrigation leads to variable flooding depth (not shown). When using the automatic irrigation option water usage is not very dif-ferent from the MA option following the irrigation calendar in Table 1. Accordingly, and AU could be used here for reference (CR). Concerning NO irrigation mode, WF_B is low (100 mm on average, Table 6), and largely variable (standard deviation 90.6 mm), being null in some years (2007, and 2012, with the two highest values of WF_G, *i.e.*, of rain-fall, Fig. 2b) and WF_I clearly null. In NO mode, rice growth occurs at the expense of previous soil storage, which provides water in excess of pre-cipitation, and therefore WF_B indicates a net loss of soil moisture during growth season (in *italics* in Table 6). Specific and relative WF indicators were calculated under the AU mode (reported in Table 6), and used for comparison under climate change conditions.

3.3. Crop yield and water footprint under climate change

In Figs. 3 to 5 future temperature, precipitation, and potential evapo-transpiration ET_p (calculated with Penman–Monteith's formula) are shown, during two trimesters (seasons), spring AMJ, and summer JAS, under CR and climate change scenarios, and in Table 7 an overview is given.

On average during the growing season (mid-April to end of August) temperature is increasing under all scenarios (from 21 °C presently to 22.2 °C under RCP8.5 of CCSM4 at 2040, and 25.1 °C under RCP8.5 of ECHAM6 at 2080). Precipitation in the same season (P_g) is lower than CR under all scenarios (from 346 mm now, to 185 mm under RCP4.5

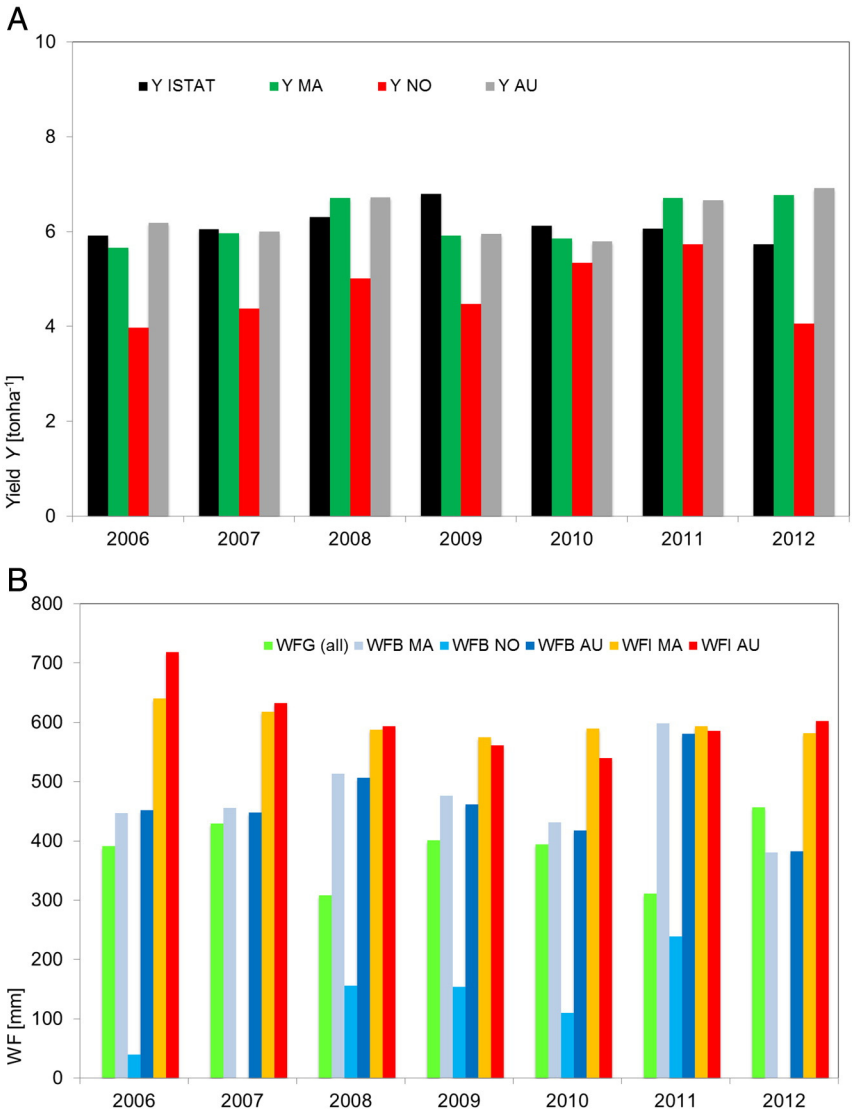

Fig. 2. Landriano. A) Accuracy of the *PC* model against ISTAT data, MA, AU, and NO irrigation modes. B) Water footprint indicators, $WF_{G,B,I}$ in all modes.

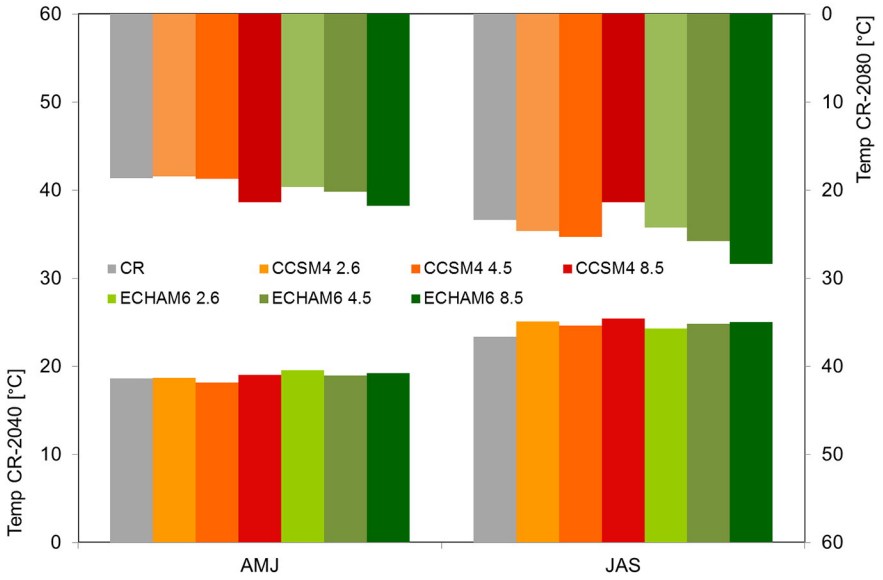

Fig. 3. Landriano. Average three-monthly temperature during the first 3 months (AMJ) and the last 3 months (JJA) of the growing season, for current reference climate (CR) and under 6 climate change scenarios (2 GCMs with 3 RCPs) at mid-century (2040, bottom) and at end-of-century (2080, top, inverted).

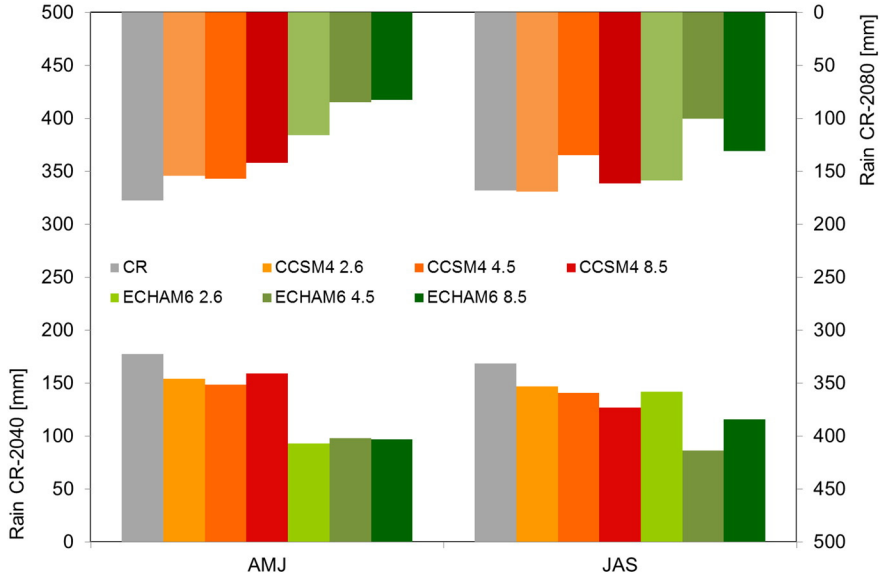

Fig. 4. Landriano. Average three-monthly precipitation during the first 3 months (AMJ) and the last 3 months (JJA) of the growing season, for current reference climate (CR) and under 6 climate change scenarios (2 GCMs with 3 RCPs) at mid-century (2040, bottom) and at end-of-century (2080, top, inverted).

of ECHAM6 at 2040, and 186 mm under the same scenario at 2080). Po-tential evapotranspiration also slightly increases (from 818 mm now, to 835 mm under of RCP8.5 of both ECHAM6 and CCSM4 at 2040, and 921 mm under RCP4.5 of CCSM4 at 2080). Fig. 6 reports projected aver-age (plus confidence limits at 95%) crop yield under climate change for Landriano. The CCSM4 model provides increasing yield under all RCPs, and for both future periods, with the sole exception of RCP8.5 at year 2080. ECHAM6 instead depict increasing yield under RCP4.5 and RCP8.5 at 2040, and decreasing elsewhere, especially at 2080. Average harvest date (D_H) (Fig. 7) is also largely variable under climate change (from day 230, *i.e.*, August 18th in the CR, to 218, *i.e.*, August 6th at 2040 under RCP2.6 of ECHAM6, and 201, or July 20th at 2080 under RCP8.5 of ECHAM6). Water footprint ($WF_{G,B,I}$) is reported in Fig. 8a, b and c. WF_G is clearly decreasing under decreasing precipitation. Accord-ingly, WF_B increases largely under all scenarios, and especially under ECHAM6, where precipitation decreases the most. Irrigation conse-quently increases, and WF_I is higher than CR everywhere (unless for RCP8.5 of CCSM4 at 2080), and most notably for ECHAM6. The average difference $WF_I - WF_B$, or irrigation excess is 101 mm (min 46 mm, ECHAM6 RCP8.5 at 2080, max 140 mm, ECHAM6 RCP2.5 at 2080), against 141 in CR, indicating on average a slightly better use of irrigation water (*i.e.*, for crop evapotranspiration) under future climate. Specific values of $WF_{G,B,I}^*$ (Fig. 9a, b and c) display a decreased use of rain water (WF_G^*), unless for CCSM4 under RCP8.5 at 2080, stemming from the decrease of precipitation under all scenarios. However, when crop yield decreases largely (as seen *e.g.*, under CCSM4 for RCP8.5 at 2080), even with decreasing precipitation WF_G^* may increase, so indicating less efficiency in use of (rain) water. Both WF_B^* and WF_I^* decrease for CCSM4 (unless at 2080 under RCP8.5), and increase for ECHAM6, ac-cording to yield variation (Fig. 6), implying that under CCSM4 increased yield would increase water use efficiency, and conversely so for ECHAM6. Analysis of $WF_{G,B,I}^P$ (Fig. 9a, b, c, WF_G being always one due to full use of rainfall here) is also interesting. $WF_{B,I}^P$ always increases (with the sole exception of CCSM4, RCP8.5 at 2080 for WF_I^P, equal to CR in practice), due to the combined decrease of rainfall, and increase of irrigation.

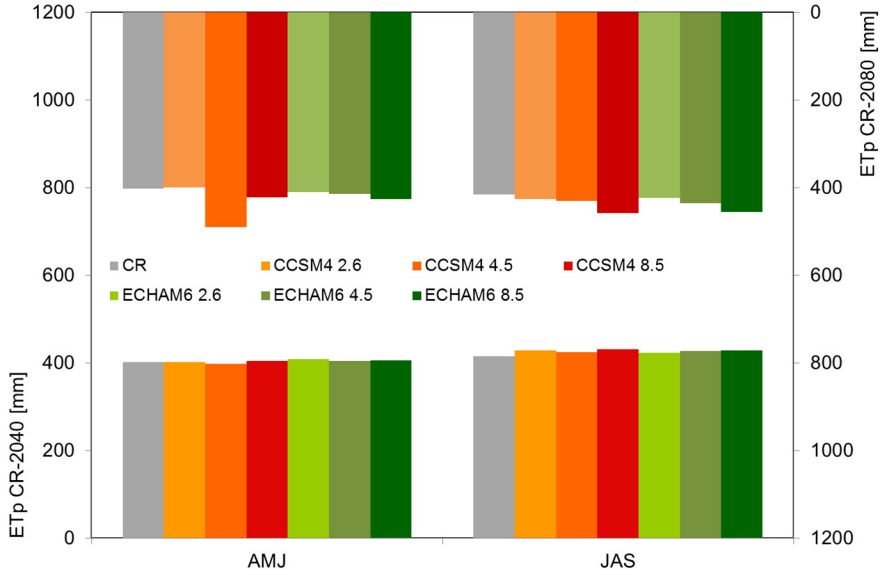

Fig. 5. Landriano. Average three-monthly evapotranspiration during the first 3 months (AMJ) and the last 3 months (JJA) of the growing season, for current reference climate (CR) and under 6 climate change scenarios (2 GCMs with 3 RCPs) at mid-century (2040, bottom) and at end-of-century (2080, top, inverted).

Table 7
Average values of weather variables and potential evapotranspiration during growth season (April–September) for control run (CR), and 2040, and 2080.

	CR			
Var/scen.	T_g [°C]	P_g [mm]	CO_2 [ppm]	ETp_g [mm]
CR	21.0	345.6	350	817.8
2040				
CCSM4 2.6	21.9	300.6	443.0	829.8
CCSM4 4.5	21.4	289.8	487.0	822
CCSM4 8.5	22.2	286.2	540.0	834.6
ECHAM6 2.6	21.9	235.2	443.0	832.2
ECHAM6 4.5	21.9	184.8	487.0	831.6
ECHAM6 8.5	22.1	213.0	540.0	835.2
2080				
CCSM4 2.6	21.6	322.8	426.0	826.2
CCSM4 4.5	22.0	292.2	534.0	921
CCSM4 8.5	21.4	303.6	845.0	880.8
ECHAM6 2.6	22.0	274.8	426.0	832.8
ECHAM6 4.5	23.0	185.4	534.0	849
ECHAM6 8.5	25.1	213.6	845.0	881.4

3.4. Correlation against climatic drivers

Results of the correlation analysis are in Table 8, where significant ($\alpha = 5\%$) coefficients are reported. Harvest date (D_H) is (negatively) correlated against *TAMJ*, and CO_2, and less (positively) to *PAMJ*. Visual analysis of rice growth (not shown) indicates that degree–day at harvesting (ca. 1500 °C d) is largely accumulated during spring, especially under climate change conditions, so high temperatures in spring affect harvest date. ECHAM6 displays always higher values of *TAMJ* than CCSM4 (19.2 °C *vs* 18.6 °C at 2040, and 20.6 °C *vs* 19.5 °C at 2040, see Fig. 3). As a consequence harvest date (Fig. 7) is always earlier in the future than that in CR (given increased CO_2), and earliest for ECHAM6. Yield *Y* is largely (negatively) correlated to *TAMJ*, and CO_2, and the sooner the D_H, the lower the yield. Future harvest (Fig. 6) is smaller for ECHAM6 than for CCSM4 (*i.e.*, for higher *TAMJ* of the former). Indeed, under CCSM4 at 2040 (and 2080 for RCP2.6, 4.5) *Y* increases against CR, likely as a response to increased CO_2 (*via* C_{R,CO_2}, and C_{TR,CO_2} in Eq. (5)) but *Y* is mostly smaller than CR under ECHAM6. For large values of CO_2 at 2080 (845 ppm under RCP8.5), *Y* decreases notably even for CCSM4, so leading to a negative correlation of *Y* *vs* CO_2. Accordingly, while CO_2 concentration increases biomass production, high values of CO_2 also increase temperature, thus providing sooner harvest date (Fig. 7), and smaller yield (*e.g.*, Masutomi et al., 2009). This happens because crop maturing is driven by degree day (see Degree–day at maturity in Table 5). So when temperature increases degree–days cumulate faster, and maturity occurs sooner. Under ECHAM6, higher temperatures in spring (Figs. 3, 4) would lead to lower yield than that under CCSM4, and at times smaller than CR at 2040 (and always much smaller at 2080). WF_B depends (positively) upon temperature during summer, and even more (negatively) upon precipitation during both seasons, *PAMJ* and *PJAS*. Under higher temperatures, evapotranspiration *ET* increases. *ET* is fed by precipitation (*i.e.*, WF_G), plus a share of irriga-tion (*i.e.*, WF_B). If within a given scenario, precipitation decreases (*i.e.*, WF_G decreases), WF_B has to increase to compensate for the increase of *ET*. During summer the projected increase of temperature is higher than that during spring (on average, in spring, +0.3 °C, and +1.4 °C, at 2040 and 2080 respectively, and in summer, +1.5 °C, and +1.6 °C, at 2040 and 2080 respectively), and potential evapotranspiration in-creases accordingly (Fig. 5). Therefore, WF_B (*i.e.*, required amount of water to meet ET_g need) increases more proportionally during summer. Clearly, lack of rain during both seasons (Fig. 4) calls for increased irriga-tion, and WF_B. At 2040, ECHAM6 displays lower *TJAS* than CCSM4 on av-erage (24.7 °C *vs* 25.05 °C), but it also displays much lower precipitation on both seasons (*PAMJ* 96 mm *vs* 154 mm, *PJAS* 115 mm *vs* 138 mm), thus requiring a larger WF_B (Fig. 8b). At 2080 ECHAM6 displays higher temperatures than CCSM4 (*TJAS* 26.1 °C *vs* 23.8 °C), together with lower rainfall (*PAMJ* 96 mm *vs* 151 mm, *PJAS* 130 mm *vs* 155 mm), so attaining again larger WF_B (Fig. 8b). Similarly to WF_B, WF is related (negatively) to rainfall during both seasons. However, WF_I does not de-pend upon temperature. While WF_B is tightly linked to *ET*, driven by temperature (*i.e.*, for ET_p) and precipitation (*i.e.*, for water availability), WF_I is only partly linked to *ET*, being mostly influenced by flooding requirements. Accordingly WF_I depends more on precipitation, in a lack of which flooding would need be maintained artificially.

4. Discussion

4.1. Accuracy of crop modeling, and WF estimates

The *PC* model, simpler than other state of the art models (*e.g.*, *CS*, *WARM*, *WOFOST*, Confalonieri et al., 2006, 2009), reproduced acceptably well rice cropping in Landriano. The *Bias* in biomass estimation was

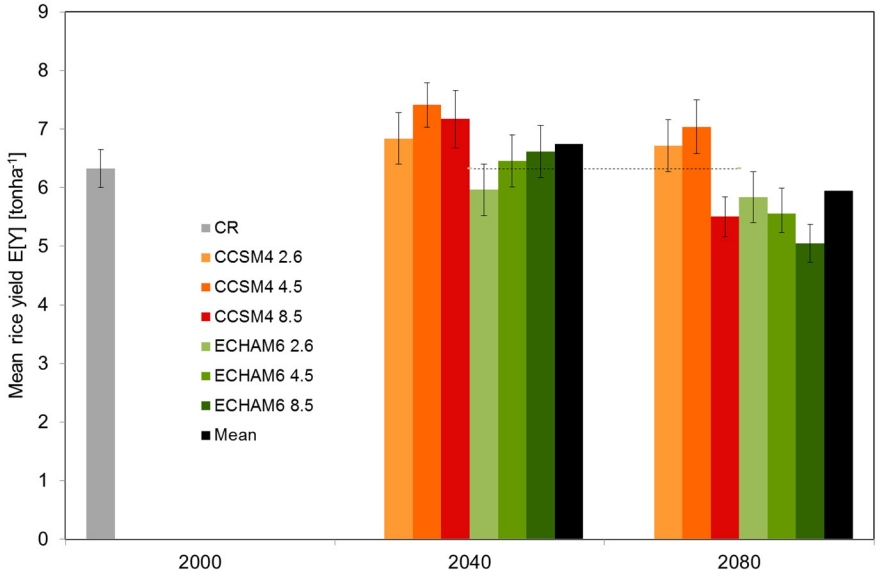

Fig. 6. Landriano. Mean rice yield, with confidence limits ($\alpha = 5\%$), CR and climate change scenarios (2 GCMs with 3 RCPs) at mid-century (2040) and at end-of-century (2080).

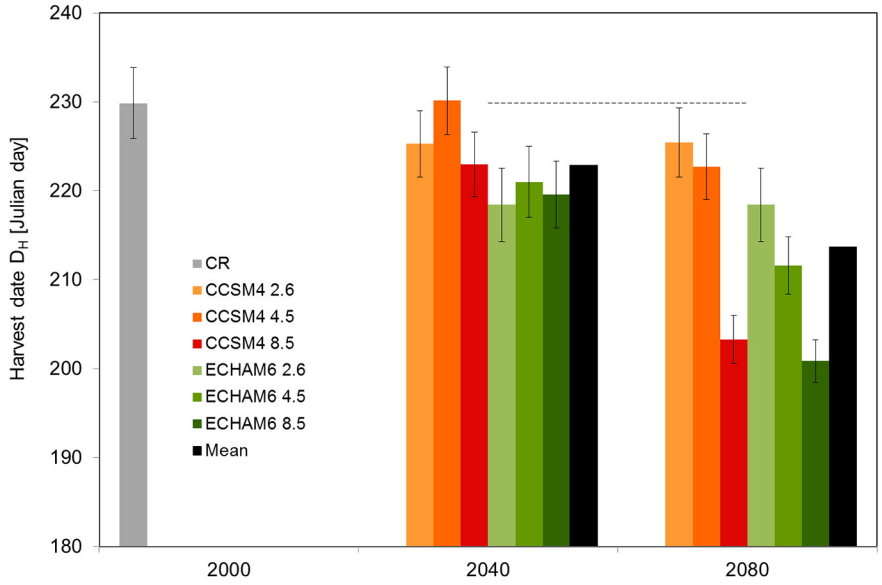

Fig. 7. Landriano. Mean harvest date, with confidence limits ($\alpha = 5\%$), CR and climate change scenarios (2 GCMs with 3 RCPs) at mid-century (2040) and at end-of-century (2080).

small (+1%, and +3%, MA and AU modes, respectively, see Table 6), and *RMSE* was acceptable (0.6 ton ha^{-1}, both MA, and AU). Inaccuracies (*RMSE*$_{\%}$) nearby 20% are accepted in crop growth simulation (*e.g.*, Cho et al., 2007), and *PC* performed within this range (10% with both MA, and AU modes). The yearly variability of the yearly Crop yield (coeffi-cient of variation, CV) was reasonably well reproduced (Obs, 0.06, *PC* 0.08, and 0.07, MA, and AU modes respectively), important for *food se-curity* assessment under (changing?) climate conditions (Torriani et al., 2007). For comparison, Confalonieri et al. (2009) validated the *WARM*, *CropSyst* and *WOFOST* models for paddy rice (*Oryza sativa* L.) growth modeling in 7 sites of the Po valley. Their *RMSE* (wet biomass) varied between 0.68 ton ha^{-1} and 2.54 ton ha^{-1}, against an average yield (wet biomass) from 10 to 17 ton ha^{-1} (here, *RMSE* = 1.1 ton ha^{-1} in AU mode, with an average yield of 11.71 ton ha^{-1}, wet biomass). Calculation of water footprint of rice at present (Fig. 2b) provides some hints. The green water footprint WF_G is on average (E[.], see Table 6) of $E[WF_G] = 384.9$ mm (standard deviation, $DEVST[WF_G] = 56.2$ mm) for both MA, and AU. Blue water footprint is also similar, *i.e.*, $E[WF_B] = 471.7$ mm, and 464.3 mm for MA, and AU ($DEVST[WF_B] = 68.8$, 64.0 mm, respectively). Irrigation footprint WF_I is also similar (Table 6, $E[WF_I] = 598.2$, 605.1 mm, for MA and AU re-spectively, $DEVST[WF_I] = 23.1$, and 58.1 mm, MA, and AU, with MA ir-rigation more constant given the fixed irrigation calendar, Table 1). Accordingly, one has on average $E[WF_I] - E[WF_B] = 126.6$ mm, and 140.8 mm for MA, and AU respectively. This would represent the excess of irrigation, *i.e.*, a quantity of water not actually used for evapotranspi-ration. As a comparison for the (specific) water footprint estimates for rice here, one can use the values from some recent estimates (Chapagain and Hoekstra, 2010, 2011). With specific reference to Italy, Chapagain and Hoekstra (2010) report (page 40; Chapagain and Hoekstra, 2010) an estimated water footprint of $WF_G = 389$ mm and $WF_B = 359$ mm, acceptably close to the estimates here, albeit with *ca.* 100 mm more for WF_B. However, Chapagain and Hoekstra (2010) calcu-late WF_B with a slightly different method than here (page 11; Chapagain and Hoekstra, 2010), so this mismatch seems acceptable, also consider-ing the site specific value here. Mom (2007) calculates rice water foot-print (called therein CWU, crop water use, page 99), for several countries worldwide, including Italy. Therein, one has $WF_G = 301$ mm, and $WF_B = 474$ mm, acceptably close to the estimates here.

Concerning specific water footprint (Fig. 9a, b, c) one has $E[WF_G^*] = 613$ kg kg^{-1}, $WF_B^* = 736$ kg kg^{-1}, and $WF_I^* = 960$ kg kg^{-1} in CR. Using yield estimates for rice in Italy from Chapagain and Hoekstra (2011) and Mom (2007), respectively of $Y = 6.10$, 6.04 ton ha^{-1}, one has approximately ($E[WF^*] \approx E[WF]/E[Y]$) $E[WF_G^*] = 637$ and 498 kg kg^{-1}, $E[WF_B^*] = 589$ and 784 kg kg^{-1}, different but substantially including the estimates here. Specific irrigation water WF_I^* is larger than the specific blue water footprint on average, and specific excess of irrigation is $E[WF_I^*] - E[WF_B^*] = 224.5$ kg kg^{-1} (AU, Table 6). Here in AU mode, during the growth season, one has $E[Q_g] = 60$ mm, and $E[Q_s] = 67$ mm, the latter mostly after crop maturity when the water layer is depleted. The average excess of irrigation is calculated as $E[WF_I] - E[WF_B] = 605 - 464 = 141$ mm. By subtracting runoff ($Q_s + Q_g$) one has $141 - 60 - 67$ mm $= 14$ mm, the average amount of water increasing soil water content locally. Cumulated Q_s amounts to $67/141 = 47\%$ of excess irrigation ($WF_I - WF_B$). When considering also percolation Q_g, on average the total runoff $Q_s + Q_g$ amounts to $127/141 = 90\%$ of excess irrigation. By taking for reference a flooding depth of 50 mm, this amounts on average to $50/141 = 35\%$ of the excess of irrigation ($WF_I - WF_B$). Accordingly, irrigation in excess is used for *ca.* 35% to maintain flooding, the rest being released through runoff (surface and percolation, *ca.* 55%), and kept as soil moisture (ca. 10%). This is a clear indication to farmer of the implications of irrigation of rice with flooding in this area. According to Chapagain and Hoekstra (2011) the excess of irrigation with respect to (blue) evapotranspiration, $WF_I - WF_B$ is not an actual water footprint, but rather it is returned into the hydrological cycle. This water may be however polluted due to manure, *i.e.*, with a gray water footprint.

4.2. Variable rice yield and WF under future climate

Future rice growth under potential climate change is variable here, and so is use of water. Uncertainty dwells into the future trends of pre-cipitation in the area, subject of a considerable debate. Among others, Brunetti et al. (2006) studied the presence of trends of yearly precipita-tion PCUM in the greater alpine region (GAR), including the case study area here, using long term observations from 192 stations. Landriano here is within their region South-East (EOF-2 in their Fig. 4), where decreasing PCUM is found. Faggian and Giorgi (2009) have studied

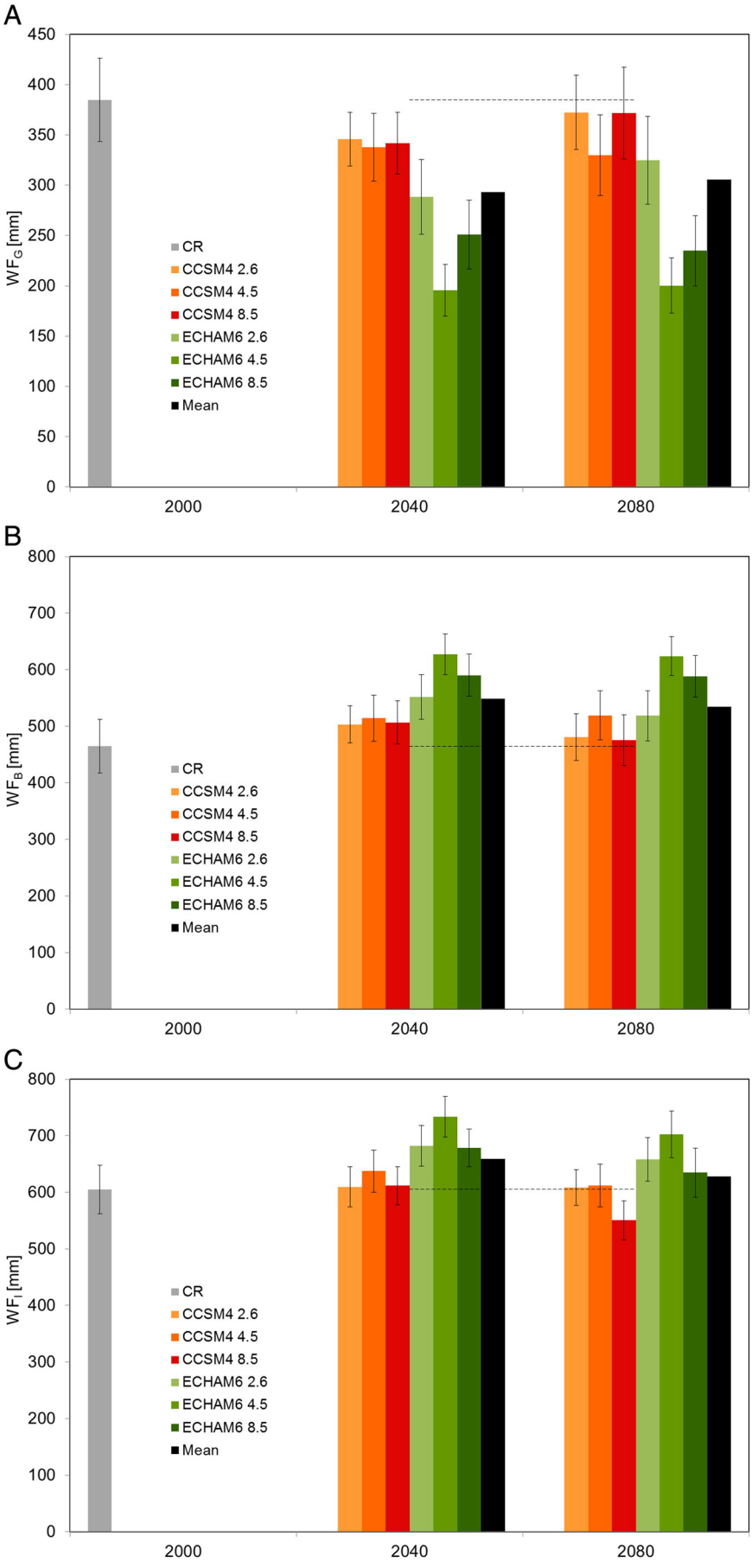

Fig. 8. Landriano. Mean water footprint, with confidence limits ($\alpha = 5\%$), CR and climate change scenarios (2 GCMs with 3 RCPs) at mid-century (2040) and at end-of-century (2080). A) Green. B) Blue. C) Irrigation.

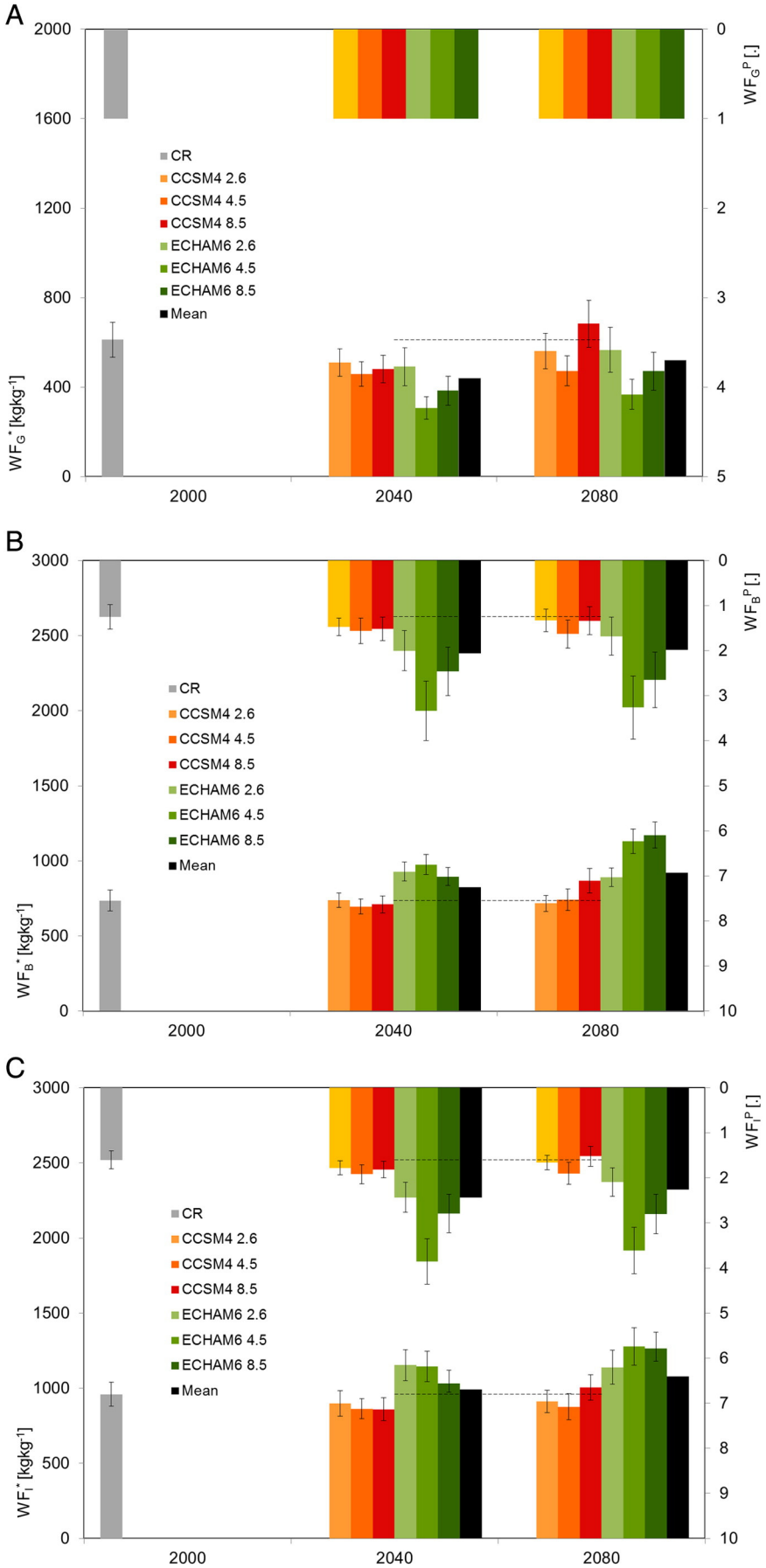

Fig. 9. Landriano. Mean water footprint specific (bottom) and relative (top, inverted), with confidence limits ($\alpha = 5\%$), CR and climate change scenarios (2 GCMs with 3 RCPs) at mid-century (2040) and at end-of-century (2080). A) Green. Relative green water footprint WFGP is always one, *i.e.*, it coincides with precipitation. B) Blue. C) Irrigation.

Table 8
Correlation analysis of key crop variables against climate descriptors, temperature (T) and precipitation (P) in spring (AMJ) and summer (JAS). Bold values indicate significance at correlation coefficients and italic indicate significance at p-values.

	TAMJ	*TJAS*	*PAMJ*	*PJAS*	CO_2	D_H	*Y*	WF_B	WF_I
TAMJ	1	*0.32*	*0.03*	*0.42*	*0.00*	*0.00*	*0.00*	*0.19*	*0.36*
TJAS	0.14	1	*0.07*	*0.06*	*0.31*	*0.28*	*0.39*	*0.02*	*0.10*
PAMJ	**−0.54**	−0.44	1	*0.01*	*0.15*	*0.01*	*0.01*	*0.00*	*0.00*
PJAS	−0.06	−0.46	**0.62**	1	*0.35*	*0.29*	*0.49*	*0.00*	*0.00*
CO_2	**0.85**	0.15	−0.32	−0.12	1	*0.00*	*0.03*	*0.29*	*0.16*
D_H	**−0.98**	−0.17	**0.60**	0.17	**−0.87**	1	*0.00*	*0.11*	*0.45*
Y	**−0.89**	−0.09	**0.62**	0.01	**−0.54**	**0.85**	1	*0.14*	*0.37*
WF_B	0.27	**0.56**	**−0.88**	**−0.90**	0.17	−0.37	−0.32	1	*0.00*
WF_I	−0.11	0.38	**−0.73**	**−0.76**	−0.30	0.04	−0.10	**0.86**	1

recent projections of precipitation supplied from 20 different GCM model (including Parallel Climate Model (PCM), Hadley Center Model version 3 (HadCM3), ECHAM5 and CCSM3 for the greater alpine region (GAR) until 2100. With reference to period 1961–90, the authors report possible variations (A1B, A2, B1 storylines of IPCC) of PCUM for the decade 2045–2054 ranging between −10% and +10% approximately, with a variability reaching −15% in Italy, strongly inhomogeneous in space (*e.g.*, Fig. 5; Faggian and Giorgi, 2009). Po valley is clearly indicated therein as a hotspot for possible climatic droughts, and until 2071–2100 the authors project a strong reduction (−30% to −50% *vs* 1961–1990) of total precipitation during spring and summer. Faggian and Giorgi (2009) also projects (2050) an average increase of temperature of *ca.* +2 °C (vs 1961–1990) for the GAR, and again they find a hotspot in the Po valley (+2–3 °C during spring for 2071–2100, +5–6 °C in summer for 2071–2100).

Further to the modified yield values *Y*, one finds (Fig. 6) increased yearly variability, as given by confidence limits for *Y* ($\alpha = 5\%$). The variability so expressed ranges from 5.1% now to 7.8% at 2080 (ECHAM6 RCP2.5), but always higher than CR (5.2%), but for CCSM4 under RCP2.6. As a consequence of the crop and water dynamics above, efficiency of water use may decrease. WF_B^* would increase on average (all scenarios) by 12% at 2040, and by 25% at 2080, indicating a larger investment of water for rice cropping. WF_I^* would increase by 3% at 2040, and by 12% at 2080. Relative WF^P indicates the amount of water needed for irrigation beyond rainfall directly falling upon the crop area. In the simplifying assumption that rainfall be constant over a given area, and that it can be entirely conveyed for irrigation (*i.e.*, no infiltration) during the growth season, if one has *e.g.*, 1 ha cultivated nowadays, he may provide water by capturing rainfall from its cultivated land ($WF_G^P = 1$), and further integrating with 1.6 ha for irrigation ($WF_I^P = 1.6$), for a total of 2.6 ha ($WF_G^P + WF_I^P = 2.6$). Under the future scenarios here, one would have on average at 2040 $E[WF_I^P] = 2.43$, *i.e.*, with the use of 3.43 ha, and at 2080 $E[WF_I^P] = 2.26$, with use of 3.26 ha. Clearly, a larger effort will likely be needed in the future to gather the required irrigation amount for rice cropping.

Albeit some studies have been carried out aimed at assessing the potential impact of climate change on crop growth and water use in sev-eral countries worldwide (Penning de Vries et al., 1990; Penning de Vries, 1993; Tubiello et al., 2000; Olesen and Bindi, 2002; Matthews and Wassmann, 2003; Parry et al., 2004; Erda et al., 2005; Olesen et al., 2007; Schmidhuber and Tubiello, 2007; Masutomi et al., 2009; Gornall et al., 2010; Ouda et al., 2010; Soussana et al., 2010; Bocchiola et al., 2013; Palazzoli et al., in press) little, if any information is available concerning future rice growth and water use in Italy, and elsewhere. Among others, Matthews and Wassmann (2003) review some studies concerning potential effect of climate change upon rice cropping. They report, among others about Penning de Vries et al. (1990), Penning de Vries et al. (1990) and Penning de Vries (1993), who used the MACROS crop simulation model, finding that a doubling of the CO_2 (*vs* pre-industrial level, *i.e.*, to 500 ppm or so) would increase yield by 10–15%, but that this would be offset by rise in temperatures, similarly to here. Erda et al. (2005) used the PRECIS model to predict the rice yield for China until 2090, under the A2 and B2 storylines of SRES (CO_2 of 721 ppm, +3.9 °C and 561 ppm, +3.2 °C). They found that yield increased under the A2 emission scenario (+8% at 2080) and decreased (−5% at 2080) under the B2 emission scenario, and CO_2 offsets yield a decrease caused by higher temperatures. Masutomi et al. (2009) assessed the impact of climate change on rice production in several countries of Asia inputting climate scenarios until 2080s from GCMs for three storylines of SRES (18 GCMs for A1B, 14 GCMs for A2, and 17 GCMs for B1) into the M-GAEZ model. They calculated the average change of production (ACP), standard deviation of the change in pro-duction (SDCP), and probability of a production decrease (PPD) for each SRES storyline. In the 2020s, they found high values of PPD for all SRES scenarios, because the negative impacts of warming were larger than the positive effects of CO_2. In the 2080s, the scenario with the highest CO_2, A2 (735 ppm) showed a notable decrease in production (−10% on average) and a high PPD in the 2080s compared with the others. In addition, A2 had the largest SDCP among the SRES scenarios. The scenario with the lowest atmospheric CO_2 concentration at 2080, B1 (541 ppm) showed a small decrease in production (−0.5% on average), a much smaller SDCP and a much lower PPD than A2. They concluded that a reduction in CO_2 emissions in the long term has great potential not only to mitigate decreases in rice production, but also to reduce crop variability, and to insure *food security*. Gornall et al.(2010) report among others a chart by Easterling et al. (2007), displaying the sensitivity of rice (mid- to high-latitude) as a result of 69 studies. At mid-latitudes, an increase from +1 °C to +3 °C would lead to substantially unchanged yield, while for changes until +5 °C yield may drop down to −30%. Adaptation may make up for climate change until +4 °C or so.

The results of the correlation analysis in Table 8 underline the specific links between climate, rice yield, and water footprint, intuitively arguable but requiring a quantitative analysis. Yield suffers from high temperatures especially in spring, and increased CO_2 may increase bio-mass only initially. WF_B required for evapotranspiration is especially high when high temperatures show up in summer, and also irrigation WF_I required for flooding increases when low precipitation occurs during the whole growth season. This findings provide guidance to i) interpret the different results from different GCMs, especially with re-spect to uncertainties in precipitation supply, and ii) define the expect-ed trends of yield and WF under different evolving climate conditions.

4.3. Limitations and future developments

Some drawbacks of this study may be objects of future investigation. The *PC* model makes a number of simplifying assumptions, most nota-bly availability of nutrients is hypothesized. Future developments of the model should therefore include nutrients' dynamics. Here, the effect of several drivers under climate change was not considered, most nota-bly of extreme events, nor they have been considered changes in pests and diseases. No gray water footprint was accounted for here, which will need to be studied in the future. Also, here it was assumed that be-sides the changing climate all other factors would remain constant in the future. Indeed, in the future agricultural practice may change, also to adapt to a changing climate, including change of sowing periods, use of different, slower maturing cultivars, and of different watering strategies (*i.e.*, without flooding). These adaptation strategies may save crop yield (see *e.g.*, Tubiello et al., 2000 for adaptation strategies for maize and wheat cropping in central and southern Italy, and

Moriondo et al., 2010 for a European wide assessment), while possibly reducing water use. Specifically for rice, irrigation without flooding (or with limited flooding periods) may provide decreased water use, still saving yield (Cabangon et al., 2004). Here, preliminary simulations carried out with *PC* for Landriano without flooding (using AU mode to mimic the effect of sprinkler irrigation, keeping soil wet enough to avoid large stress, RWC > 95%) showed that lack of flooding may provide smaller water use (in the order of −22% or so, $E[WF_I]$ = 472 mm, *vs* $E[WF_I]$ = 605 mm with flooding), with a loss of yield of −3% or so on average, but down to −12% (*vs* the same year during 2006–2012) in some cases due to thermal stress, with increasing variability of yield (down to −12% *vs* the mean value, *vs* −8% with flooding now). Howev-er, site specific experiments are needed to assess rice growth without flooding. In the future, the *PC* model will be used to focus on specific adaptation measures for rice cropping and water use in the Po valley, which need to be carried systematically, requiring effort beyond the present paper. Eventually, the results here seem to be of interest, and they provide i) a methodology to assess crop growth and water use under given climate conditions, and ii) a believable conjecture concerning future rice yield and water consumption until the end of XXI century in the Po valley of Italy, where crop management under climate change must be tackled soon enough. Recent studies have demonstrated that transient climate change within the present century will likely lead to decreased summer flows from rivers in the Italian Alps (Groppelli et al., 2011a; Confortola et al., 2013; Bocchiola, 2014), possi-bly limiting water availability for irrigation. Moreover, evidence is being raised that future WF of crops in this area will increase (*e.g.*, maize, Bocchiola et al., 2013), so strategies for monitoring, modeling, and de-creasing large scale water consumptions are necessary.

5. Conclusions

Site specific water footprint in the Po valley of Italy was assessed using the *PolyCrop* model. Future yield and water use under climate change until the end of the century were investigated. The results depend upon the specific GCM, and RCP, and large variability is seen. However, there is agreement about some key points, namely i) increased CO_2 concentration may lead to constant or increased rice yield until mid-century, at the cost of increased water use, but ii) at the end of the century rice yield would likely decrease under largely increased temperature, and yet water use would further increase. Accordingly adaptation strategies will be necessary to maintain acceptable rice yield, and water consumption, under increasing demand and modified climate conditions. The template built here is usable for i) crop (rice) yield assessment ii) evaluation of water requirements, and iii) testing of optimal adaptation strategies under climate change, and represents a relevant contribution for water resource management, especially to the ongoing debate about *food security* in Europe and worldwide.

Acknowledgments

Eng. Ester Nana, and Eng. Marika Merletti are kindly acknowledged for their support in the *PC* set-up and use. Support from the "*SHARE-Stelvio*" project funded by Lombardia Region, and from "5xMille:I-CARE" project funded by Politecnico di Milano are also kindly acknowledged. The two anonymous reviewers are acknowledged for delivering useful suggestions to improve the paper.

References

Adams, R.M., Hurd, B.H., Lenhart, S., Leary, N., 1998. Effects of global climate change on agriculture: an interpretative review. Clim. Res. 11, 19–30.
Addimando, N., Nana, E., Bocchiola, D., 2014. Modelling pasture dynamics in a Mediterranean environment: a case study in Sardinia region, Italy. J. Irrig. Drain. Eng. 04014063 http://dx.doi.org/10.1061/(ASCE)IR.1943-4774.0000818.
Allan, T., 1993. Fortunately There Are Substitutes for Water: Otherwise Our Hydropolitical Futures Would Be Impossible, Paper Presented at Conference on Priorities for Water Resources Allocation and Management. Overseas Dev. Admin., London.
Bocchi, S., Castrignanò, A., 2007. Identification of different potential production areas for corn in Italy through multitemporal yield map analysis. Field Crop Res. 102 (3), 185–197.
Bocchiola, D., 2014. Long term (1921–2011) hydrological regime of Alpine catchments in Northern Italy. Adv. Water Resour. 70, 51–64.
Bocchiola, D., Diolaiuti, G., Soncini, A., Mihalcea, C., D'Agata, C., Mayer, C., Lambrecht, A., Rosso, R., Smiraglia, C., 2011. Prediction of future hydrological regimes in poorly gauged high altitude basins: the case study of the upper Indus, Pakistan. Hydrol. Earth Syst. Sci. 15, 2059–2075.
Bocchiola, D., Nana, E., Soncini, A., 2013. Impact of climate change scenarios on crop yield and water footprint of maize in the Po valley of Italy. Agric. Water Manag. 116, 50–61. Brouwer, F.M., 1988. Determination of broad-scale land use changes by climate and soils. Working Paper WP-88-007. International Institute for Applied Systems Analysis, Laxenburg, Austria.
Brunetti, M., Maugeri, M., Nanni, T., Auer, I., Böhm, R., Schöner, W., 2006. Precipitation variability and changes in the greater Alpine region over the 1800–2003 period. J. Geophys. Res. 111, D11107. http://dx.doi.org/10.1029/2005JD006674.
Cabangon, R.J., Tuong, T.P., Castillo, E.G., Bao, L.X., Lu, G., Wang, G., Cui, Y., Bouman, B.A., Li, Y., Chen, C., Wang, J., 2004. Effect of irrigation method and N-fertilizer management on rice yield, water productivity and nutrient-use efficiencies in typical lowland rice conditions in China. Paddy Water Environ. 2, 195–206.
Campbell, G.S., 1985. Transport models for soil–plant systems. Development in Soil Science 14. Elsevier, Amsterdam.
Chapagain, A.K., Hoekstra, A.Y., 2010. The green, blue and grey water footprint of rice from both a production and consumption perspective. UNESCO-IHE, Value of Water, Research Report Series No. 40.
Chapagain, A.K., Hoekstra, A.Y., 2011. The blue, green and grey water footprint of rice from production and consumption perspectives. Ecol. Econ. 70 (4), 749–758.
Cho, M.A., Skidmore, A.C.F., van Wieren, S.E., Sobhan, I., 2007. Estimation of green grass/herb biomass from airborne hyperspectral imagery using spectral indices and partial least squares regression. Int. J. Appl. Earth Obs. Geoinf. 9, 414–424.
Confalonieri, R., Bechini, L., 2004. A preliminary evaluation of the simulation model *CropSyst* for alfalfa. Eur. J. Agron. 21, 223–237.
Confalonieri, R., Bocchi, S., 2005. Evaluation of CropSyst for simulating the yield of flooded rice in northern Italy. Eur. J. Agron. 23, 315–326.
Confalonieri, R., Mariani, L., Bocchi, S., 2005. Analysis and modelling of water and near water temperatures in flooded rice (*Oryza sativa* L.). Ecol. Model. 183, 269–280.
Confalonieri, R., Acutis, M., Bellocchi, G., Cerrani, I., Tarantola, S., Donatelli, M., Genovese, G., 2006. Exploratory sensitivity analysis of CropSyst, WARM and WOFOST: a case-study with rice biomass simulations. Ital. J. Agrometeorol. 3, 17–25.
Confalonieri, R., Acutis, M., Gianni Bellocchi, G., Donatelli, M., 2009. Multi-metric evaluation of the models WARM, CropSyst and WOFOST for rice. Ecol. Model. 220 (11), 1395–1410.
Confalonieri, R., Bregaglio, S., Rosenmundc, A.S., Acutis, M., Savin, I., 2011. A model for simulating the height of rice plants. Eur. J. Agron. 34, 20–25.
Confortola, G., Soncini, A., Bocchiola, D., 2013. Climate change will affect water resources in the Alps: a case study in Italy. J. Alp. Res. RGA/JAR 100–103 (http://rga.revues.org/2176).
Cure, J.D., Acock, B., 1987. Crop responses to carbon dioxide doubling: a literature survey. Agric. For. Meteorol. 38, 127–145.
Donatelli, M., Stockle, C., Ceotto, E., Rinaldi, M., 1997. Evaluation of *CropSyst* for cropping systems at two locations of northern and southern Italy. Eur. J. Agron. 6, 35–45.
Easterling, W., Apps, M., 2005. Assessing the consequences of climate change for food and forest resources: a view from the IPCC. Clim. Chang. 70 (1–2), 165–189.
Easterling, W.E., et al., 2007. Food, fibre and forest products. In Climate change 2007: impacts, adaptation and vulnerability. In: Parry, M.L., Canziani, O.F., Palutikof, J.P., Linden, P.J.V.D., Hanson, C.E. (Eds.), Contribution of Working Group II to the Fourth Assessment Report of the Intergovernmental Panel on Climate Change. Cambridge University Press, Cambridge, UK, pp. 273–313.
Erda, L., Wei, X., Hui, J., Yinlong, J., Yue, L., Liping, B., Liyong, X., 2005. Climate change impacts on crop yield and quality with CO_2 fertilization in China. Philos. Trans. R. Soc. B 360, 2149–2154.
Fader, M., Gerten, D., Thammer, M., Lotze-Campen, H., Lucht, W., Cramer, W., 2011. Internal and external green–blue agricultural water footprints of nations, and related water and land savings through trade. Hydrol. Earth Syst. Sci. 15, 1641–1660.
Faggian, P., Giorgi, F., 2009. An analysis of global model projections over Italy, with particular attention to the Italian Greater Alpine Region (GAR). Clim. Chang. http://dx.doi. org/10.1007/s10584-009-9584-4.
FAO, 2009. Adapting to climate change. In Unasylva 60 (231/232).
Fava, F., Parolo, G., Colombo, R., Gusmeroli, F., Della Marianna, G., Monteiro, A.T., Bocchi, S., 2010. Fine-scale assessment of hay meadow productivity and plant diversity in the European Alps using field spectrometric data. Agric. Ecosyst. Environ. 137 (1–2), 151–157.
Ferrero, A., 2006. Challenges and opportunities for a sustainable rice production in Europe and Mediterranean area (Preface). Paddy Water Environ. 4 (1), 11–12.
Gent, P.R., et al., 2011. The Community Climate System Model Version 4. J. Clim. 24, 4973–4991.
Gornall, J., Betts, R., Burke, E., Clark, R., Camp, J., Willett, K., Wiltshire, A., 2010. Implications of climate change for agricultural productivity in the early twenty-first century. Philos. Trans. R. Soc. B 365, 2973–2989.
Groppelli, B., Bocchiola, D., Rosso, R., 2011a. Spatial downscaling of precipitation from GCMs for climate change projections using random cascades: a case study in Italy. Water Resour. Res. 47, W03519. http://dx.doi.org/10.1029/2010WR009437.

Groppelli, B., Soncini, A., Bocchiola, D., Rosso, R., 2011b. Evaluation of future hydrological cycle under climate change scenarios in a mesoscale Alpine watershed of Italy. NHESS 11, 1769–1785. http://dx.doi.org/10.5194/nhess-11-1769-2011.
Hoekstra, A.Y. (Ed.), 2003a. Virtual Water Trade: Proceedings of the International Expert Meeting on Virtual Water Trade, Delft, The Netherlands, 12–3 December 2002, Value of Water Research Report Series No. 12. UNESCO-IHE, Delft, The Netherlands.
Hoekstra, A.Y., 2003b. Virtual Water: An Introduction. UNESCO-IHE, Delft, The Netherlands.
Hoekstra, A.Y., Chapagain, A.K., 2008. Globalization of Water: Sharing the Planet's Freshwater Resources. Blackwell Publishing, Oxford, UK.
Hoekstra, A.Y., Hung, P., 2005. Globalisation of water resources: international virtual water flows in relation to crop trade. Glob. Environ. Chang. 15, 45–56.
IPCC, 2013. Summary for policymakers. In: Stocker, T.F., Qin, D., Plattner, G.-K., Tignor, M., Allen, S.K., Boschung, J., Nauels, A., Xia, Y., Bex, V., Midgley, P.M. (Eds.), Climate Change 2013: The Physical Science Basis. Contribution of Working Group I to the Fifth Assessment Report of the Intergovernmental Panel on Climate Change. Cambridge University Press, Cambridge, United Kingdom and New York, NY, USA.
Jarvis, A.J., Mansfield, T.A., Davies, W.J., 1999. Stomatal behaviour, photosynthesis and transpiration under rising CO_2. Plant Cell Environ. 22, 639–648.
Leuning, R., 1995. A critical appraisal of a combined stomatal photosynthesis model for C3 plants. Plants Cell Environ. 18, 357–364.
Masutomi, Y., Takahashi, K., Harasawa, H., Matsuoka, Y., 2009. Impact assessment of climate change on rice production in Asia in comprehensive consideration of process/parameter uncertainty in general circulation models. Agric. Ecosyst. Environ. 131, 281–291.
Matthews, R., Wassmann, R., 2003. Modelling the impacts of climate change and methane emission reductions on rice production: a review. Eur. J. Agron. 19, 573–598.
Mekonnen, M.M., Hoekstra, A.Y., 2011. The green, blue and grey water footprint of crops and derived crop products. Hydrol. Earth Syst. Sci. 15, 1577–1600.
Mom, R.J.C., 2007. A High Spatial Resolution Analysis of the Water Footprint of Global Rice Consumption (Master Thesis) University of Twente, Enschede, The Netherlands.
Monteith, J.L., 1977. Climate and the efficiency of crop production in Britain. Philos. Trans. R. Soc. B281, 277–294.
Moriondo, M., Bindi, M., Kundzewicz, Z.W., McEvoy, D., Wreford, A., 2010. Impact and adaptation opportunities for European agriculture in response to climatic change and variability. Mitig. Adapt. Strateg. Glob. Chang. 15, 657–679.
Morrison, J.I.L., 1987. Intercellular CO_2 concentration and stomatal response to CO_2. In: Zeiger, E., Cowan, I.R., Farquhar, G.D. (Eds.), Stomatal Function. Stanford University Press, Stanford, pp. 229–251.
Morrison, J.I.L., 1999. Interactions between increasing CO_2 concentration and temperature on plant growth. Plant Cell Environ. 22 (6), 659–682.
Nana, E., Corbari, C., Bocchiola, D., 2014. A hydrologically based model for crop yield and water footprint assessment: study of maize in the Po valley. Agric. Syst. 127, 139–149.
O'leary, G.J., Christy, B., Nuttall, J., Huth, N., Cammarano, D., Stockle, C., Basso, B., Shcherbak, I., Fitzgerald, G., Luo, Q., Farre-Codina, I., Palta, J., Asseng, S., 2015. Response of wheat growth, grain yield and water use to elevated CO_2 under a Free-Air CO_2 Enrichment (FACE) experiment and modelling in a semi-arid environment. Glob. Chang. Biol. 21, 2670–2686. http://dx.doi.org/10.1111/gcb.12830.
Olesen, J.E., Bindi, M., 2002. Consequences of climate change for European agricultural productivity, land use and policy. Eur. J. Agron. 16, 239–262.
Olesen, J.E., Carter, T.R., Diaz-Ambrona, C.H., Fronzek, S., Heidmann, T., Hickler, T., Holt, T., Minguez, M.I., Morales, P., Palutikof, J.P., Quemada, M., Ruiz-Ramos, M., Rubæk, G.H., Sau, F., Smith, B., Sykes, M.T., 2007. Uncertainties in projected impacts of climate change on European agriculture and terrestrial ecosystems based on scenarios from regional climate models. Clim. Chang. 81, 123–143.
Ouda, S.A., Khalil, F.A., El Afandi, G., Ewis, M.M., 2010. Using CropSyst model to predict barley yield under climate change conditions in Egypt: I. Model calibration and validation under current climate. Afr. J. Sci. Biotechnol. 4, 1–5.
Palazzoli, I., Maskey, S., Uhlenbrook, S., Nana, E., Bocchiola, D., 2014. Impact of prospective climate change upon water resources and crop yield in the Indrawati basin, Nepal. Agric. Syst. http://dx.doi.org/10.1016/j.agsy.2014.10.016 (in press, November 2014).
Parry, M.L., Rosenzweig, C., Iglesias, A., Livermore, M., Fischer, G., 2004. Effects of climate change on global food production under SRES emissions and socio-economic scenarios. Glob. Environ. Chang. 14, 53–67.
Pearch, R.W., Bjorkman, O., 1983. Physiological effects. In: Lemon, E.R. (Ed.), CO_2 and Plants, The Response of Plants to Rising Levels of Atmospheric CO_2. Westview Press, Boulder, Colorado, pp. 65–105.
Peel, M.C., Finlayson, B.L., McMahon, T.A., 2007. Updated world map of the Köppen–Geiger climate classification. Hydrol. Earth Syst. Sci. 11, 1633–1644.
Penning de Vries, F.W.T., 1993. Rice production and climate change. In: Penning de Vries, F.W.T., Teng, P., Metselaar, K. (Eds.), Systems Approaches for Agricultural Development. Kluwer Academic Publishers, Dordrecht, The Netherlands, pp. 175–189.
Penning de Vries, F.W.T., van Keulen, H., van Diepen, C.A., Noy, I.G.A.M., Goudriaan, J., 1990. Simulated yields of wheat and rice in current weather and in future weather when ambient CO_2 has doubled. Climate and Food Security, International Rice Research Institute, Los Baños, Philippines, pp. 347–358.
Richter, G.M., Acutis, M., Trevisiol, P., Latiri, K., Confalonieri, R., 2010. Sensitivity analysis for a complex crop model applied to Durum wheat in the Mediterranean. Eur. J. Agron. 32 (2), 127–136.
Rosenzweig, C., Hillel, D., 1998. Climate Change and the Global Harvest. Oxford University Press, New York.
Rossi, S., Rampini, A., Bocchi, S., Boschetti, M., 2010. Operational monitoring of daily crop water requirements at the regional scale with time series of satellite data. J. Irrig. Drain. Eng. ASCE 136 (4), 225–231.
Rost, S., Gerten, D., Bondeau, A., Lucht, W., Rohwrer, J., 2008. Agricultural green and blue water consumption and its influence on the global water system. Water Resour. Res. 44, W09405 (17 pp.).
Schmidhuber, J., Tubiello, F.N., 2007. Global food security under climate change. PNAS 104 (50), 19703–19708.
Soussana, J.F., Graux, A.I., Tubiello, F.N., 2010. The use of modeling for projections of climate change impacts on crops and pastures. J. Exp. Bot. 61 (8), 2217–2228.
Stevens, B., et al., 2013. Atmospheric component of the MPI-M Earth System Model: ECHAM6. J. Adv. Model. Earth Syst. 5, 1–27.
Stöckle, C.O., Nelson, R., 1999. Cropping Systems Simulation Model User's Manual. Washington State University (http://www.sipeaa.it/tools/CropSyst/CropSyst_manual.pdf).
Stöckle, C.O., Williams, J.R., Rosenberg, N.J., Jones, C.A., 1992. A method for estimating the direct and climatic effects of rising atmospheric carbon dioxide on growth and yield of crops: part I/modification of the EPIC model for climate change analysis. Agric. Syst. 38, 225–238.
Stöckle, C.O., Martin, S., Campbell, G.S., 1994. Cropsyst, a cropping systems model: water/nitrogen budgets and crop yield. Agric. Syst. 46, 335–359.
Stöckle, C., Donatelli, M., Roger, N., 2003. CropSyst, a cropping systems simulation model. Eur. J. Agron. 18, 289–307.
Strzepek, K., Boehlert, B., 2010. Competition for water for the food system. Philos. Trans. R. Soc. B 365, 2927–2940.
Supit, I., van Diepen, C.A., de Wit, A.J.W., Kabat, P., Baruth, B., Ludwig, F., 2010. Recent changes in the climatic yield potential of various crops in Europe. Agric. Syst. 103, 683–694.
Tanner, C.B., Sinclair, T.R., 1983. Efficient water use in crop production. In: Taylor, H.M., Jordan, W.R., Sinclair, T.R. (Eds.), Limitation to Efficient Water Use in Crop Production. American Society of Agronomy, Madison, pp. 1–27.
Torriani, D., Calanca, P., Lips, M., Amman, H., Beniston, M., Fuhrer, J., 2007. Regional assessment of climate change impacts on maize productivity and associated production risk in Switzerland. Reg. Environ. Chang. 7, 209–221.
Tubiello, F.N., Donatelli, M., Rosenzweig, C., Stockle, C., 2000. Effects of climate change and elevated CO_2 on cropping systems: model predictions at two Italian sites. Eur. J. Agron. 13, 179–189.
Tubiello, F.N., Soussana, J.F., Howden, S.M., 2007. Crop and pasture response to climate change. PNAS 104 (50), 19686–19690.